*Journal of the European Ceramic Society* **13** (1994) 265–273

# Characterization of Agglomerate Strength of Coprecipitated Superfine Zirconia Powders

J. L. Shi, Z. X. Lin, W. J. Qian & T. S. Yen

State Key Laboratory of High Performance Ceramics and Superfine Microstructure, Shanghai Institute of Ceramics, Chinese Academy of Sciences, 1295 Ding Xi Road, Shanghai 200050, People's Republic of China

(Received 18 May 1993; revised version received 30 October 1993; accepted 10 November 1993)

***Abstract***

*The compaction behaviour of nano sized zirconia powders prepared by the coprecipitation method was studied by means of pore size distribution measurements and density versus pressure relation determination. Agglomerate strength can be characterized with the determination of pressure dependence of compacted density and pore size distributions of compacts. By combining these two techniques it was found that there were two strength points for agglomerates, one of lower pressure at which agglomerates began to fragment and another one of higher pressure at which agglomerates were fully fragmented. The strength point for complete agglomerate fragmentation was much more useful for characterizing the properties of agglomerates.*

*Das Verdichtungsverhalten von Nano Zirkonium oxid, hergestellt durch eine Koausscheidungsmethode, wurde untersucht. Die Charakterisierung des Materials erfolgte durch die Bestimmung der Porengrößenverteilung und der Dichte Druck Beziehung. Die Festigkeit der Agglomerate kann aus der Druckabhängigkeit der Dichte und der Porengrößenverteilung bestimmt werden. Aus der Verbindung dieser beiden Techniken ergaben sich zwei Festigkeitspunkte für die Agglomerate, der erste, bei niedrigem Druck, bei dem der Zerfall der Agglomerate einsetzt und ein zweiter, bei hohem Druck, bei dem die Agglomerate vollständig zerfallen sind. Der zweite Punkt ist für die Charakterisierung der Agglomerateigenschaften wesentlich nützlicher.*

*On a étudié la compaction de poudres de zircone nanométriques, préparées par coprécipitation, en observant la distribution de tailles des pores et en mesurant la densité en fonction de la pression. La variation de la distribution de tailles et de la densité du matériau compacté avec la pression permet de caractériser la résistance des agrégats. En continuant ainsi ces deux techniques, on trouve deux points caractéristiques de la résistance des agrégats: l'un, à basse pression, correspond au moment où les agrégats commencent à se fragmenter, l'autre, à pression plus élevée, correspond à la fragmentation complète de ces agrégats. La valeur de la résistance lors de la fragmentation complète s'est révélée la plus adéquate pour caractériser les agrégats.*

## 1 Introduction

Powder properties have a major effect on the sintering behaviour and microstructural development[1–4] and thus the performance of ceramic materials. The agglomerates, which are inevitably present in fine powders, are of vital importance in influencing powder performance during compaction and sintering. Agglomerates can be characterized by their geometrical and physical properties. The geometrical properties of agglomerates, including their content, size and size distributions, which can be determined by scanning electron microscopy (SEM) or the sedimentation technique, are preliminary facets of the agglomeration state,[5] but even more important is agglomerate strength,[6] which is decisive in powder performance.[8–10] Agglomerate strength determines the compaction behaviour and therefore the sinterability, of powders. If agglomerates are completely fragmented during compaction, a compacted green sample will contain no agglomerates, despite a large amount of agglomerates present in the starting powder,[11] and the sintering behaviour of green samples thus would not be affected by the agglomerates contained in powders. Agglomerates that can be fragmented easily are weak. Strong agglomerates cannot be broken during compaction, and both the compacts containing these strong agglomerates and inter agglomerate



*Journal of the European Ceramic Society* 0955-2219/94/$7.00 

pores would show poor sinterability[12] and microstructure develops even if agglomerate content is low and inter agglomerate pore size is small.[10]

Agglomerate strength can be characterized with the determination of compaction density versus pressure logarithm relations and it was proposed by Niesz and coworkers,[6,7] and followed by Reed and coworkers,[13,14] Dynys & Halloran[11] and Roosen,[16] that the intersection ($P_y$) of two linear portions (see Fig. 1) in the density versus pressure relation is the agglomerate strength (defined as the apparent yielding point of agglomerates in this paper). However, this point is only the one at which agglomerates begin to break down, which leads to faster increase of density with the increase of pressure, but not the one at which all agglomerates are eliminated. Even if at a pressure larger than $P_y$, inter agglomerate pores[13,14] can still be present in compacts. The investigations made by Niesz and Reed and their coworkers were focused on spray dried alumina powders, the agglomerates were artificial granules and the agglomerate properties were affected by the binder properties. However in chemically processed zirconia powders, agglomerates are formed during processing and the agglomerate properties may be much different from those in spray dried alumina powders.[10,11]

Most recently, Ge *et al.*[17] reported that a gradual transition region from the low pressure linear portion to higher-pressure linear portion ('a concave upward portion in the middle' between the linear portion—as claimed by the authors) of the density versus pressure logarithm relation corresponds to the fragmentation processes of the agglomerates. Unfortunately their formula derivation from eqn (4) to eqn (5) was not correct even if the agglomerate is incompressible, as assumed by the authors (which in fact meant that the agglomerate can not be crushed, in contrast to their result in Fig. 5 in their paper), the 'net volume of powder' ($V'_m$) could not be replaced by $V_m + V'_a$ ($V'_a$ here is the pore volume within agglomerates[17] simply because the particle and agglomerate were both incompressible, as assumed by the authors. Therefore the calculated results shown in Fig. 5 in their paper based on their incorrect assumption and formula derivation do not tell the truth. As a matter of fact, this gradual transition only shows the scattering or distribution of agglomerate strength $P_y$ at the beginning of fragmentation.

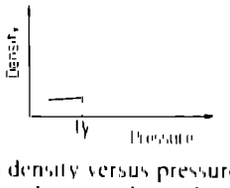


**Fig. 1.** Compaction density versus pressure logarithm relation of agglomerated powders.[6,7]

The present study investigates the compaction behaviour of superfine coprecipitated zirconia powders by determining the pressure dependence of compaction density and pore size distribution, and two strength points were found useful for characterizing the agglomerate strength.

## 2 Experimental Procedure

The starting powders were prepared by coprecipitation routes using zirconium oxychloride and yttrium nitrate as raw materials. The mixed solution of zirconium oxychloride and yttrium nitrate was added to an ammonia solution, which resulted in coprecipitation, and the final pH value was kept ~9.5. The coprecipitates were washed with distilled water (repeated more than ten times) to remove anions. The washed cake was then treated differently. Powder S-1 was prepared by a subsequent ethanol wash (repeated more than six times) to replace water until the water content in filtrates was less than 4%. Powder S-2 was prepared by two subsequent ethanol washes to replace water partially (water content in filtrates about 30%) for YSZ powders, (7 mol% $Y_2O_3$, 3 mol% $Y_2O_3$) but for Y-TZP powder direct dispersion with ultrasonic treatment for more than 30 min of the water washed coprecipitates was employed. The two batches of powder were then dried in an oven at 110 °C overnight. Finally, powder S-3 was obtained by spray drying the dilute aqueous suspension of the coprecipitates (the solid content based on zirconia in suspension was about 5 wt%), in a mini spray drier using a two fluid atomizer[18] (Brinkman and Buchi 190) for YSZ powder or in a large spray drier with a pressure atomizer for Y-TZP powder. The obtained zirconium hydroxides were approximately spherically shaped. The spray drying temperatures were 220–230 °C and 110–120 °C at inlet and outlet respectively. The dried powders were calcined at various temperatures from 420 °C to 1000 °C to produce zirconia powders.

The pore size distributions of powder compacts obtained by first die pressing and/or followed by cold isostatic pressing at different pressures were determined by mercury porosimetry (Micromeritics 9110), by assuming the contact angle between zirconia and mercury of 130° and the surface tension of mercury of 0.485 N/m. The accuracy of intrusion volume and the pressure of mercury can be ensured as these two parameters are so easy to measure and control. The detectable minimum pore size (diameter) was 3 nm at the maximum intrusion pressure. The compaction behaviour was determined by carefully measuring the compaction densities at various pressures *in situ* during compaction, and the

compaction densities were calculated with the data of compact weight, die diameter used and the piston displacements, which was measured by a dial gauge, during compaction. No binders were added in powders for compaction. To avoid pressure inhomogeneity, upper and lower pistons were both movable, the die was polished and fully lubricated with oil acid, and the thickness to diameter ratios of compacts were kept less than 1:5.

## 3 Results

### 3.1 Primary particle and agglomerate micrographs and pore size distributions

Figure 2 shows the primary particle micrographs (TEM) of Y-TZP powders calcined at 750 °C for 120 min. It can be seen that the particles of powder S-1 are nano-sized and well dispersed, while those of powder S-3 are much larger sized and strongly agglomerated.[19,20] Such a situation for YSZ powders was very similar except for the difference of primary particle size.

Agglomerate micrographs were observed with SEM, as shown in Fig. 3 for powder S-3 for Y-TZP and YSZ, respectively. The spray dried spherical agglomerates were too strong to be dispersed with ultrasonic treatment before subjecting to the micrographs observation. The agglomerate sizes were different, depending on the spray drying methods, but two kinds of agglomerates were both very strong as the spray drying conditions were similar (e.g. temperature, solid contents in suspension).

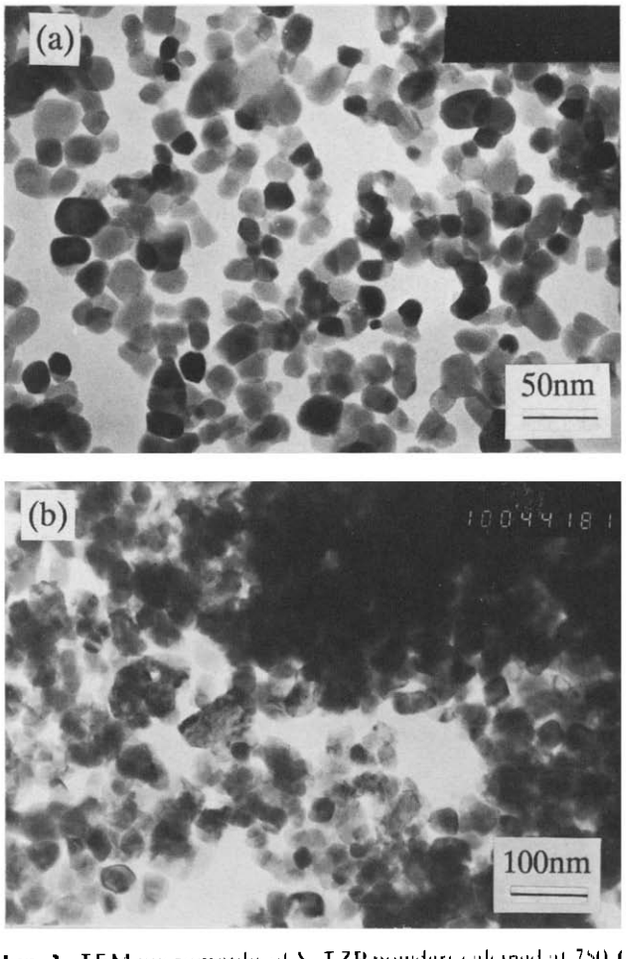


**Fig. 2.** TEM micrographs of Y-TZP powders calcined at 750 °C for 120 min: (a) powder S-1 and (b) powder S-3.

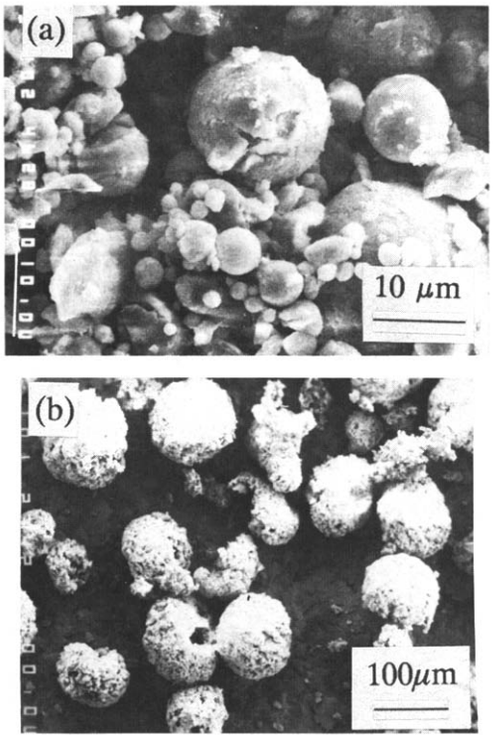


**Fig. 3.** SEM micrographs of agglomerates of (a) YSZ powder S-3 and (b) Y-TZP powder S-3.

The pore size distributions of powders calcined at various temperatures shows that there were inter-primary particle pores and inter-agglomerate pores.[11] These two kinds of pores have been defined as primary pores and secondary pores in the authors' previous paper,[11] respectively, and this paper follows this usage. Figure 4 is a typical example of powder S-2. Pores less than 80 nm were thought to be inter-primary particle pores (i.e. primary pores) and the other larger pores were inter-agglomerate pores (i.e. secondary pores). The pore size distribution of powder S-1 was similar to that of powder S-2.

### 3.2 Pore size distribution compacts

*3.2.1 Pore size distribution of powders S-1*

Figure 5 shows the pore size distributions of

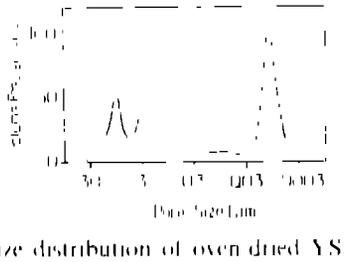

**Fig. 4.** Pore size distribution of oven-dried YSZ powder S-2 calcined at 600 °C.

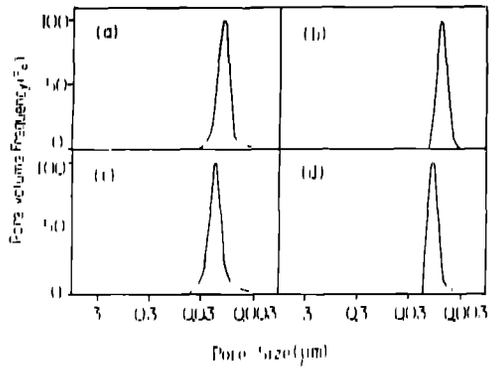


**Fig. 5.** Pore size distributions of the compacts S-1 of (a) YSZ, 100 MPa; (b) YSZ, 250 MPa; (c) Y-TZP, 100 MPa and (d) Y-TZP, 250 MPa.

powders S-1 at 100 MPa and 250 MPa. It can be seen that even at pressure as low as 100 MPa, agglomerates were totally fragmented, both for YSZ and Y-TZP powders. Higher pressure at 250 MPa only leads to diminished pore volume and pore size. Calcination from 420 to 1000 °C did not affect the compaction behaviour of powder S-1.[11]

*3.2.2. Pore size distribution of powders S-2*

*3.2.2.1. Pressure dependence.* Figure 6 shows the pore size distributions of 600 °C calcined YSZ powder S-2 at different compaction pressures. At 50 MPa, the compact contained some secondary pores larger than those at 100 MPa. The compact formed under higher pressure, 200 MPa, showed no agglomerates remained in the compact, as can be seen in Fig. 7, which shows the relationship between pore volume

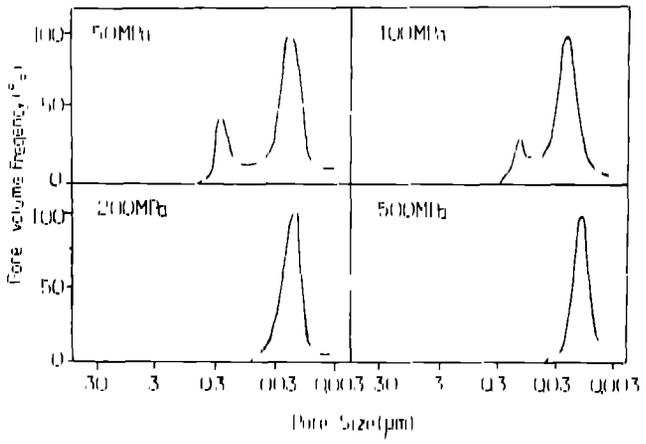


**Fig. 6.** Pore size distributions of 600 °C calcined YSZ powder compacts S-2 at different pressures.

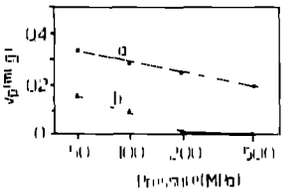


**Fig. 7.** Pressure dependence of the pore volume of YSZ powder compacts S-2: (a) primary pore volume and (b) secondary pore volume.

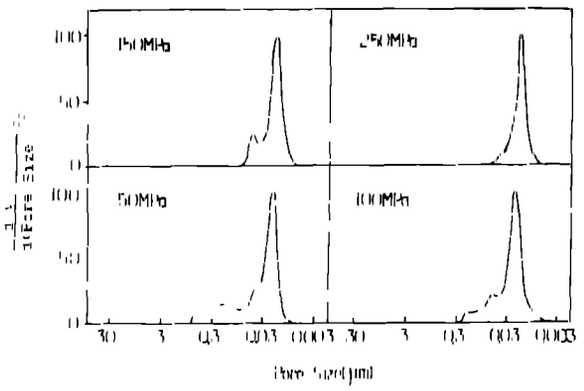


**Fig. 8.** Pore size distributions of 750 °C calcined Y-TZP powder compacts S-2 at different pressures.

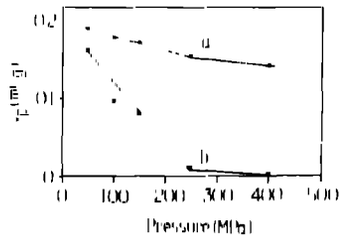


**Fig. 9.** Pressure dependence of the pore volume of Y-TZP powder compacts S-2: (a) primary pore volume and (b) secondary pore volume.

and pressure. A similar relationship was also true for Y-TZP powder (750 °C calcined) as shown in Fig. 8. At 250 MPa the secondary pores were nearly completely eliminated, as can be seen in Fig. 9.

*3.2.2.2. Calcination temperature dependence.* Figure 10 shows the pore size distributions of the compacts at 100 MPa for YSZ powders S-2 calcined at different temperatures. Calcination temperature affects the secondary pore volume and size in compacts, as shown in Fig. 11. Agglomerates formed by calcination at 1000 °C were very hard and not influenced even at 500 MPa, as shown in Fig. 12.

*3.2.3. Pore size distribution of powder compacts S-3.* Secondary pores were much less affected by compaction pressure for powder S-3. Figure 13 shows the

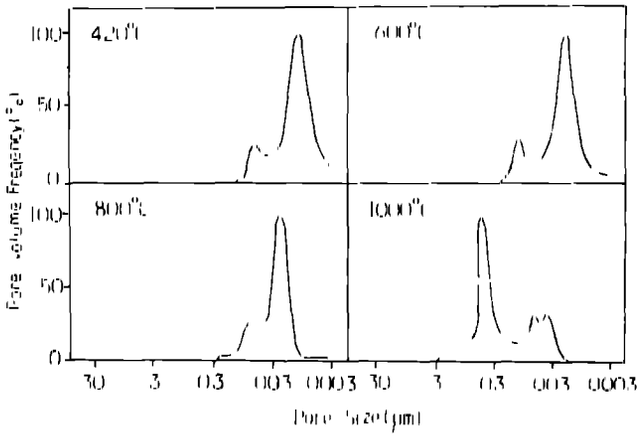


**Fig. 10.** Pore size distributions of the compacts at 100 MPa for YSZ powder S-2 calcined at different temperatures.

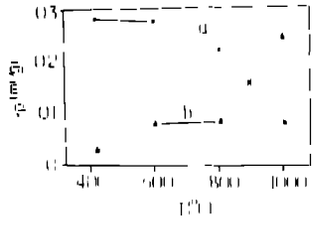

Fig. 11. Temperature dependence of pore volumes in YSZ powder compacts S 2: (a) primary pore volume and (b) secondary pore volume

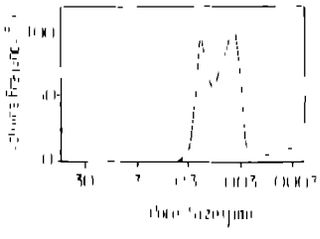

Fig. 12. Pore size distribution of YSZ powder S 2 calcined at 1000 °C and compacted at 500 MPa

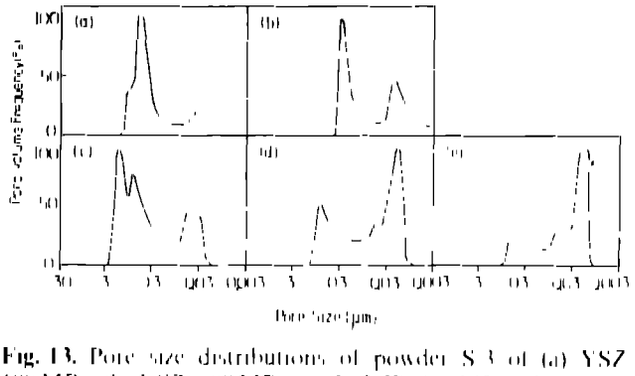

Fig. 13. Pore size distributions of powder S 3 of (a) YSZ 100 MPa, (b) YSZ 500 MPa, (c) Y TZP 100 MPa, (d) Y TZP 250 MPa and (e) Y TZP 500 MPa

pore size distributions of the compacts of YSZ and Y TZP powders S 3 at different pressures. Hard agglomerates were present in powder compacts S 3 even at 500 MPa, both for Y TZP and YSZ powders.

### 3.3 Density versus pressure relations

Figures 14 and 15 show the relationship between compaction density and pressure logarithm for YSZ and Y TZP powders. It can be seen that in the pressure ranges used, there are three linear regions[13] and two intersections in the relations. However, the three regions are different for differently agglomerated powders. For powder S 1 and S 2 the slope of region III is smaller than that of region II while for powder S 3 the situation is reversed. The different compaction responses to pressure was related to the different agglomerate properties.

In region I compacts densified by agglomerates rearrangement and the first intersection at lower pressure ($P_y$) was the point for agglomerates to begin to fragment (i.e. apparent yielding point). In region II compacts densified by the fragmentation of agglomerates, e.g. by the elimination of both secondary pores and primary pores, as shown by the increase of

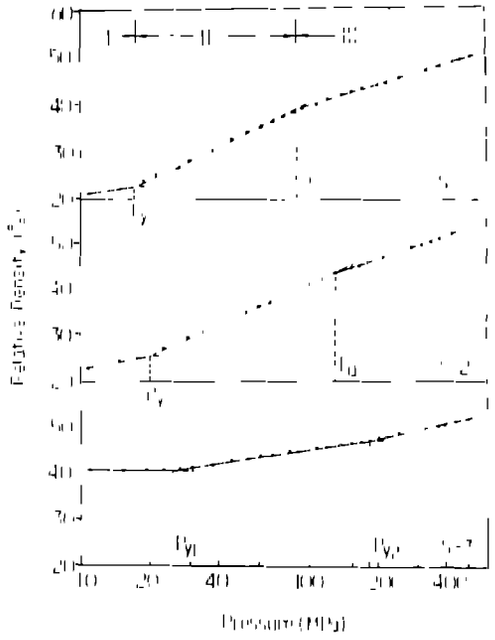

Fig. 14. Compaction density versus pressure logarithm relations for YSZ powders

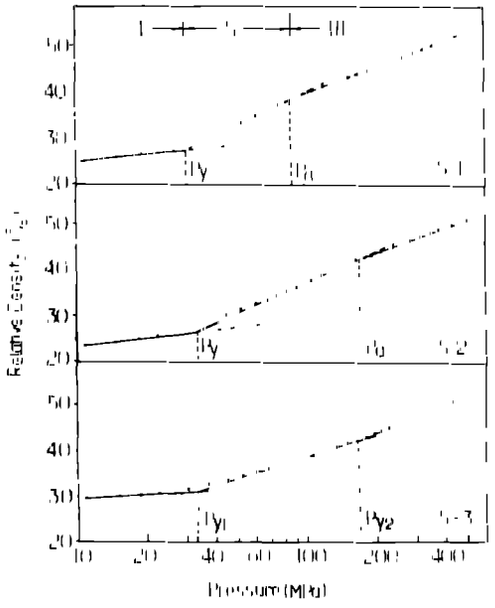

Fig. 15. Compaction density versus pressure logarithm relations for Y TZP powders

the line slope from region I to region II. In this region the relation between density and pressure can be written as[13]

$$D_2 = D_y + m_2 \ln P / P_y \qquad (1)$$

where $P$ is pressure, $D_2$ is compact density in region II, $D_y$ is the density when $P = P_y$, and $m_2$ is the line slope of this region. For powders S 1 and S 2 the second intersection at higher pressure ($P_y$) means the total fragmentation of agglomerates (i.e. apparent fragmentation point), so in region III, after the elimination of secondary pores, the densification was achieved only by the removal of primary pores[14]

$$D_3 = D_a + m_3 \ln P / P_a \qquad (2)$$

where $D_1$ is the compact density in region III, $D_a$ is the density when $P = P_a$ and $m_3$ is the line slope in region III. As no secondary pores were present in this region the line slope in region III was smaller than that in region II, i.e. $m_3 < m_2$.

For powder S-3, the increased line slope of region II to region III shows the fragmentation of hard agglomerates and elimination of secondary pores in this region, and the second intersecting point of $P_{s2}$ is the apparent yielding point of the hard agglomerates in powder S-3. So for the powders composed of hard agglomerates, the density versus pressure relations can be written as

$$D_2 = D_{s1} + m'_2 \ln P / P_{s1} \tag{3}$$

for region II, and

$$D_3 = D_{s2} + m'_3 \ln P / P_{s2} \tag{4}$$

for region III, where $D_{s1}$ and $D_{s2}$ are the densities at intersecting points of $P_{s1}$ and $P_{s2}$. As in region II densification was accompanied only by agglomerate rearrangement and sliding, while in region III both the removal of secondary and intra-agglomerate (i.e. primary) pores contributed to the densification process, so $m'_3 < m'_2$.

### 3.4 Micrographs of the compacts

Figure 16 is the SEM micrographs of differently processed Y-TZP powder compacts at different forming pressures. The microstructures of the compacts were homogeneous and no micro-sized pores (i.e. secondary pores) are visible. In contrast, large agglomerates and secondary pores were present in the compacts for S-3 even at 500 MPa. Figure 17 is the SEM micrographs at a higher amplifying magnitude than Fig. 16.

## 4 Discussion

### 4.1 Agglomerate content calculation with pore size distribution data

Assuming the distribution peaks of various kinds of pores can be distinguished, and the packing densities of agglomerate and primary particles are $P_p$ and $P_a$, respectively, then as particle volume is proportional to the corresponding pore volume under a certain packing density, the agglomerate content ($C_{agg}$) can be calculated as follows:

$$\begin{aligned} C_{agg} &= \frac{\text{Volume of agglomerated primary particles}}{\text{Volume of total primary particles}} \\ &= \frac{\text{Intraagglomerate primary pore volume}}{\text{Volume of total primary pores}} \\ &= \frac{(1 - P_p)\cdot \text{Volume of agglomerates}}{\text{Volume of total primary pores}} \\ &= \frac{(1 - P_p)P_a \cdot \text{Volume of secondary pores } (V_s)}{(1 - P_a) \cdot \text{Volume of total primary pores } (V_p)} \end{aligned} \tag{5}$$

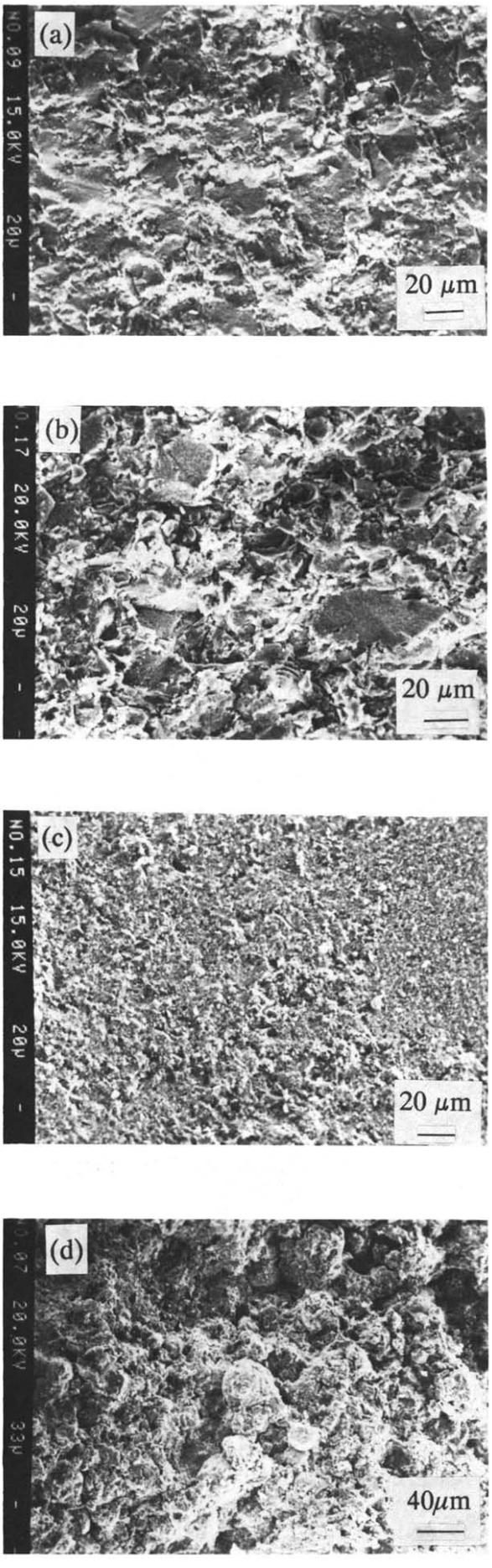


**Fig. 16.** SEM micrographs of Y-TZP powder compacts of (a) S-1, 100 MPa, (b) S-2, 100 MPa, (c) S-2, 250 MPa and (d) S-3, 500 MPa

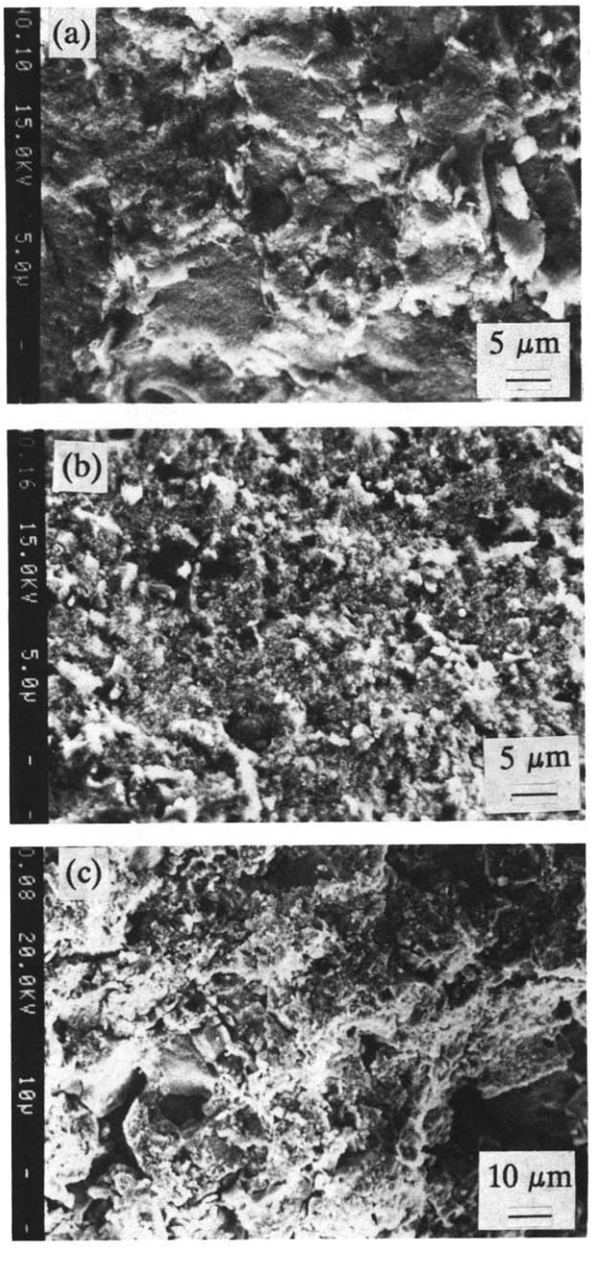


**Fig. 17.** SEM micrographs at higher amplifying magnitudes than Fig. 16 (a) S 1, 100 MPa, (b) S 2, 250 MPa and (c) S 3 500 MPa

The volume of secondary pore, $V_a$, and primary pore, $V_p$, can be determined from the pore size distribution data, and then the agglomerate content, $C_{agg}$, can be calculated

$$C_{agg} = K V_a / V_p \quad (6)$$

with

$$K = P_a(1 - P_p)/(1 - P_a) \quad (7)$$

If a 100% agglomerate content is assumed in powder calcined at 600 C, the constant $K$ in eqn (3) can be determined from the pore size distribution data in Fig. 2 as 0.588. The value of the constant can also be determined using the values of $P_a$ and $P_p$ that were calculated to be 0.46 and 0.32,[21] respectively, so the constant $K$ is 0.59.

Dependence of agglomerate contents, which was

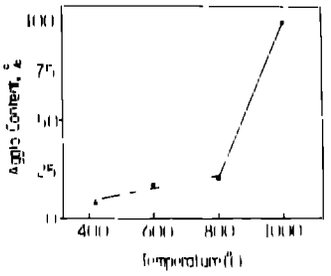


**Fig. 18.** Calculated agglomerate contents in YSZ powder compacts S 2 (100 MPa) as a function of calcination temperatures

calculated from eqn (6) in YSZ powder compacts S 2 on calcination temperature is shown in Fig. 18. Figure 19 shows the agglomerate contents in compacts S 2 as a function of forming pressure. So for the powders S 2, agglomerate contents in the compacts increased with increases in calcining temperature and decreased with increasing compaction pressure. The complete elimination of agglomerates in compaction is indicated by zero agglomerate content, where the minimum compaction pressure required is the agglomerate fragmentation strength (apparent fragmentation strength).

### 4.2 Agglomerate apparent strength: yielding and fragmentation strength

The agglomerate strength can be apparently defined by the intersections in compact density versus pressure logarithm relations. The first intersections for powders S 1 and S 2 are their agglomerate apparent yielding strength ($P_y$), indicating that at the pressure agglomerates begin to fragment. The yielding strengths for S 1 and S 2 are less than 30 MPa, or may be lower. The second intersections are their apparent fragmentation strength ($P_a$).

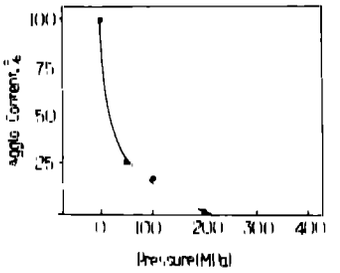


(a)

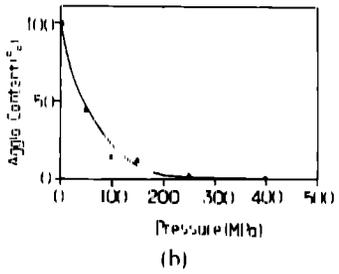


(b)

**Fig. 19.** Calculated agglomerate contents in (a) 600 C calcined YSZ and (b) 750 C calcined Y TZP powder compacts S 2 as a function of forming pressure

From Figs 14 and 15 it is known that at 100 MPa there were no agglomerates present in powder compacts S 1, so the apparent fragmentation strengths of agglomerates were not higher than 100 MPa, as verified by the pore size distribution results shown in Fig. 5. The fragmentation strength of agglomerates for powder S 2 were around 200 MPa, as confirmed by the pressure dependence of the agglomerate contents shown in Fig. 19.

Micrographic observations (Figs 16 and 17) revealed that uniform compacts could be achieved only when the forming pressure were higher than the apparent fragmentation strength, at which all secondary pores were removed.

There were two yielding pressures for powder S 3. The first one at lower pressure indicates the beginning of agglomerate rearrangement but no fragmentation takes place and the second one is the apparent yielding point for agglomerate fragmentation. The strength point for the total fragmentation of agglomerates in powder S 3 was beyond the pressure limit used, which means that the apparent fragmentation strength was larger than the pressure upper limit of 500 MPa used.

### 4.3 Agglomerate effective strength

Effective strength of agglomerates is the true strength of agglomerates. At the apparent yielding pressure the effective stress on agglomerates was equal to or a little larger than the bridging strength between primary particles within agglomerates. However, at or a little larger than the yielding pressure, agglomerates do not fragment completely and secondary pores are still present in the compacts. This is caused by increased loading area between particles and therefore decreased effective stress with increased density, as the effective stress acting on the compacts can be roughly expressed as follows

$$\sigma_{\mathrm{eff}} = P/\rho \tag{8}$$

where $P$ and $\sigma_{\mathrm{eff}}$ are the apparent (external) pressure and effective stress and $\rho$ is the relative density. For a compact containing agglomerates, both secondary and primary pores will decrease compact densities and increase the effective stress. The local effective stress were dependent on the local microstructure, however, eqn (8) is qualitatively applicable for stress analysis. With the elimination of secondary and primary pores in compacts during compaction at a certain external pressure, the effective stress acting on the compacts would increase and therefore higher external pressure is needed to compensate this decrease in effective stress and to keep the effective stress equal to or a little larger than the intrinsic bridging strength within agglomerates for further densification. As the pressure increased to a certain value when all secondary pores were removed, agglomerates were totally fragmented, the pressure is the apparent fragmentation strength ($P_a$) of agglomerates.

According to eqn (8), assuming the intrinsic bridging strength within agglomerates is $\sigma_i$, which is thought to be related to compaction pressure and or density, the apparent yielding strength $P_y$ and fragmentation pressure $P_a$ can be written as

$$P_y = \sigma_{iy}\ d_y \tag{9}$$

and

$$P_a = \sigma_{ia}\ d_a \tag{10}$$

where $\sigma_{iy}$ and $\sigma_{ia}$ are the intrinsic strength of agglomerates at yielding and fragmentation points. The detected values of apparent strength $P_y$ and $P_a$, and the calculated values of $\sigma_{iy}$ and $\sigma_{ia}$ for differently processed powders are shown in Table 1. As for apparent strength, the values of $P_y$ are much higher than for spray dried alumina,[13] whose apparent yielding strength was mainly determined by the properties of binders.[14]

## 5 Summary

Agglomerate strength of superfine coprecipitated zirconia powder was characterized with the determination of pore size distributions of compacts and the compaction behaviours (i.e. compaction density

**Table 1.** Intersection densities, apparent and intrinsic strength of agglomerates in YSZ and Y-TZP powders

| *Powder* | | *Y-TZP* | | | *YSZ* | | |
|---|---|---|---|---|---|---|---|
| | | *S 1* | *S 2* | *S 3*[a] | *S 1* | *S 2* | *S 3*[a] |
| Intersection density ($\mu$m$^{-1}$) | $d_y$ | 27 | 26 | 42 | 22 | 25 | 46 |
| | $d_a$ | 38 | 42 | 80 | 39 | 43 | 82 |
| Apparent strength (MPa) | $P_y$ | 29 | 32 | 170 | 16 | 20 | 175 |
| | $P_a$ | 90 | 185 | >500 | 90 | 140 | >500 |
| Intrinsic strength (MPa) | $\sigma_{iy}$ | 105 | 122 | 400 | 73 | 100 | 370 |
| | $\sigma_{ia}$ | 237 | 440 | >1000 | 230 | 236 | >1000 |

[a] Only $P_{y2}$ is used

versus pressure logarithm relations). The compaction behaviour of powders in the pressure range of 10–500 MPa shows that there were two strength points for characterizing the agglomerate strength: one at lower pressure was the apparent yielding strength at which agglomerates began to break down and another one of higher pressure was the apparent fragmentation strength where all agglomerates were fragmented. The intrinsic agglomerate strength was calculated according to the apparent strength. The pore size distribution measurement and the micrograph observation results of the compacts supported the conclusion.

The magnitude of the agglomerate strength, especially the fragmentation strength, was strongly related to the powder processing history, at least for chemically processed superfine powders. For superfine zirconia powders prepared by the coprecipitation method, the ethanol washing or ultrasonic dispersion of the coprecipitates may result in soft or semi-hard agglomerates which yield at about 15–30 MPa and can be fragmented completely at not higher than 100 to 250 MPa, while agglomerates prepared by spray drying the dilute coprecipitate suspension yields hard agglomerates which can not be fragmented completely even at 500 MPa.

## References


1. Lange F. F. & Metcalf M. Processing related fracture origins: I. II. III. *J. Am. Ceram. Soc.* **66**(6) (1983) 369.
2. Lange F. F. Sinterability of agglomerated powder. *J. Am. Ceram. Soc.* **65**(2) (1982) 83.
3. Rhodes, W. H. Agglomerate and particle size effect on sintering yttria-stabilized zirconia powders. *J. Am. Ceram. Soc.* **64**(1) (1981) 19.
4. Haberko K., Characteristics and sintering behavior of zirconia ultrafine powders. *Ceram. Int.* **5** (1979) 148.
5. Shi J. L. & Lin Z. X. Characterization of nano-sized zirconia powders. Accepted for Publication in *Powder Tech.* **74** (1993).
6. Niesz D. E. & Bennett R. B. Agglomerate structure and properties. In *Ceramic Processing before Firing*, ed. G. Y. Onoda Jr & L. L. Hench. John Wiley & Sons, NY, 1978, pp. 63–71.
7. Niesz D. E., Bennett R. B. & Snyder, M. Strength characterization of powder aggregates. *Am. Ceram. Soc. Bull.* **51**(9) (1972) 677.
8. Ciftioglu M., Akinc M. & Burkhart L. Effect of agglomerate strength on sintered density for yttria powders containing agglomerates of monosized spheres. *Am. Ceram. Soc. Bull.* **70**(11) (1987) 1829.
9. Dynys F. W. & Halloran J. W. Influence of agglomerates on sintering. *Am. Ceram. Soc. Bull.* **67**(9) (1984) 597.
10. Shi J. L., Gao J. H., Lin Z. X. & Yen T. S. Effect of agglomerates in superfine zirconia powder compacts on the microstructural development. *J. Mater. Sci.* **28** (1993) 342.
11. Shi J. L. Characterization of the pore size distributions in the superfine zirconia powder compacts. *J. Solid State Chem.* **95**(2) (1992) 412.
12. Shi J. L., Gao J. H., Lin Z. X. & Yen T. S. Sintering behavior of fully agglomerated ultrafine zirconia powder compacts. *J. Am. Ceram. Soc.* **74**(5) (1991) 994.
13. Lukasiewicz S. J. & Reed J. S. Characterization compaction response of spray dried agglomerates. *Am. Ceram. Soc.* **57**(9) (1978) 798.
14. Dimilia R. V. & Reed J. S. Dependence of compaction on the glass transition temperature of the binder phase. *ibid.* **62**(4) (1983) 484.
15. Dynys F. W. & Halloran J. W. Compaction of aggregated alumina powders. *J. Am. Ceram. Soc.* **66**(9) (1983) 655.
16. Roosen A. Techniques for agglomeration control during wet chemical powder synthesis. *Adv. Ceram. Mater.* **3**(2) (1988) 131.
17. Ge R., Zheng D., Zhao T. & Zhu X. Model for the characterization of agglomerated ceramic powder compaction. *Bull. Ceram. Trans.* **92**(2) (1993) [illegible].
18. Shi J. L., Gao J. H. & Lin Z. X. Preparation of YSZ powder by coprecipitation and spray drying and its effect on sintered density. *J. Chin. Ceram. Soc.* **17**(5) (1989) 417.
19. Shi J. L., Lu C. W., Kuo C. T. & Yen T. S. Determination of crystallite size of ultrafine zirconia powders as a function of calcination temperature. *Ceram. Int.* **18** (1992) [illegible].
20. Shi J. L. Crystallite growth characteristics of superfine zirconia powder. to be published.
21. Shi J. L. PhD Thesis, Preparation and properties of superfine zirconia powders, Shanghai Institute of Ceramics, Shanghai, 1989.